6.4 EXPERIMENTAL DETERMINATION OF THE TURBULENT KINETIC ENERGY BUDGET WITHIN AND ABOVE AN URBAN CANOPY

Andreas Christen[(1)]*, Mathias W. Rotach[(2)], Roland Vogt[(1)]
[(1)] University of Basel, Institute of Meteorology, Climatology and Remote Sensing, Basel, Switzerland.
[(2)] Swiss Federal Institute of Meteorology and Climatology, MeteoSwiss, Zürich, Switzerland.

1 INTRODUCTION

Many aspects of the turbulent exchange processes above rough surfaces are summarized in the budget of turbulent kinetic energy (TKE). With the increasing need of accurately predicting dispersion within and close to urban canopies for air quality, health and emergency response, detailed knowledge on the magnitude of turbulent fluctuations and the underlying physical processes that create, relocate and destroy kinetic energy become important. This may help to improve model parameterizations and to develop more appropriate scaling methods.

TKE budgets of the flow within and above plant canopies have been addressed in a number of field experiments and wind tunnel studies, and have been modeled in various large eddy simulations (LES). However, the characteristic density, the non-permeability and stiffness of buildings that form an urban canopy compared to the flexible and highly fractal structures that are present in plant canopies do not imply a direct applicability of the results from plant canopies to urban environments. Little is known on the TKE budget within the urban roughness sublayer, and there is especially a lack of experimental data on the profiles of dissipation rate and transport terms within the urban canopy layer.

In this contribution we present results from the Basel Urban Boundary Layer Experiment BUBBLE, which was carried out in the city of Basel, Switzerland (Rotach *et al.,* 2004) in 2001/02. We focus on the main tower 'Basel-Sperrstrasse', where a profile of six ultrasonic anemometer-thermometers (sonics) was operated over 9 months in and above a street canyon.

2 THEORY

Within the urban roughness sublayer, the flow is influenced by the presence of individual buildings with the consequence that turbulence statistics and flux densities are vertically and horizontally inhomogeneous (Rotach, 1999). Therefore, in analogy to plant canopies, horizontally (spatially) averaged terms are introduced into the equation of turbulent kinetic energy in order to regain horizontal homogeneity on a larger scale (Finnigan, 2000):

$$\left(\frac{\partial}{\partial t}+\langle\overline{u_j}\rangle\frac{\partial}{\partial x_j}\right)\frac{1}{2}\langle\overline{u_i'u_i'}\rangle = \underbrace{-\langle\overline{u_i'u_j'}\rangle\frac{\partial\langle\overline{u_i}\rangle}{\partial x_j}}_{Ps} \underbrace{-\langle\overline{u_i'u_j'}''\frac{\partial\langle\overline{u_i}''\rangle}{\partial x_j}\rangle}_{Pd} + \underbrace{\frac{g}{T}\langle\overline{u_3'\theta'}\rangle}_{Pb} + Pt \underbrace{-\frac{\partial\langle\overline{u_i'u_i'u_j'}\rangle/2}{\partial x_j}}_{Tt} \underbrace{-\frac{\partial\langle\overline{u_j}''\overline{u_i'u_i'}''/2\rangle}{\partial x_j}}_{Td} \underbrace{-\frac{\partial\langle\overline{p'u_j'}\rangle}{\partial x_j}}_{Tp} + \underbrace{\upsilon\frac{\partial^2\langle\overline{u_i'u_i'}\rangle/2}{\partial x_j x_j}}_{Tv} - \epsilon \quad (1)$$

Time averaging of a flow property is indicated by an overbar, a horizontal spatial average is denoted by angular brackets. Double primes denote dispersive terms, which result from deviations of the local temporal mean of a flow property from the spatial-temporal average (Raupach and Shaw, 1982). *Ps* is the conversion of resolved scale kinetic energy into TKE by wind shear and *Pd* is its dispersive part. The production (or destruction) of turbulence by buoyant effects is described by *Pb*, while *Pt* is an extra term which accounts for turbulence created by moving vehicles in the street canyon (Di Sabatino *et al,.* 2003). The locally produced turbulent kinetic energy can be vertically relocated by turbulent (*Tt*), dispersive (*Td*), viscous (*Tv*) and pressure transport of TKE (*Tp*). Finally, dissipation of turbulent kinetic energy ε is always a sink.

3 INSTRUMENTATION AND DATA

The triangular lattice tower 'Basel-Sperrstrasse' was deployed within a vegetation-free street canyon and reached up to 32 m. Amongst others, the tower supported six sonics arrayed in a vertical profile with an enhanced vertical resolution around roof top (Fig. 1, Tab. 1). This setup covers roughly the vertical domain from street level up to two times the mean building height. The canyon is located in a dense built-up part of the city with a mean building height *h* of 14.6 m and a plan area density of 0.54.

20 Hz raw data were stored from November 2001 to July 2002. The sonics were checked and intercompared in a wind tunnel before and/or after the experiment. In order to minimize flow distortion effects, instrument individual correction matrices were derived from wind tunnel runs and used to correct the wind

* *Corresponding author address:*
Andreas Christen
Institute of Meteorology, Climatology and Remote Sensing,
Department of Geosciences, University of Basel
Klingelbergstrasse 27, CH-4056 Basel, Switzerland
e-mail: andreas.christen@unibas.ch

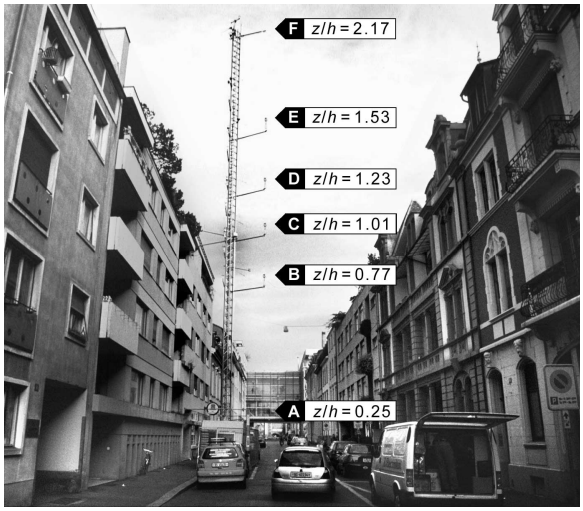

Fig. 1: The experimental tower 'Basel-Sperrstrasse' with sonic levels labelled.

Tab. 1: Turbulence instrumentation at 'Basel-Sperrstrasse' for the period Nov 2001 to July 2002.

	z (m)	z/*h*	Instrument	Sampling rate [1]	Calibration
F	31.7	2.17	Gill HS	100 / 20 Hz	Wind tunnel
E	22.4	1.53	Gill R2 A	166 / 20.8 Hz	Wind tunnel
D	17.9	1.23	Gill R2 O	166 / 20.8 Hz	Wind tunnel
C	14.7	1.01	Gill R2 O	166 / 20.8 Hz	Wind tunnel
B	11.3	0.77	Gill R2 O [2]	166 / 20.8 Hz	Manufacturer
A	3.6	0.25	Gill R2 O [2]	166 / 20.8 Hz	Manufacturer

[1] Internal / output sampling rate
[2] From May 23 to July 15, 2002 these instruments were replaced by Metek USA-1, with 40/20 Hz sampling rate (wind tunnel)

vectors (Vogt and Feigenwinter, 2004). Angles of attack where the flow distortion effects of a particular instrument are large or the tower obstructs the flow have been excluded from analysis.

Directly measuring spatial averages in a full scale experiment is nearly impossible and would require huge arrays of simultaneously measuring instruments at different locations. Instead, spatial averages can be approximated by averaging over different wind directions. Practically, all available data from an instrument have been classified into 16 different wind direction classes. For each wind direction class, an individual average of a term has been calculated. Then, by averaging over all wind direction classes (equally weighted) a global average is deduced. This average is taken as a surrogate for the real horizontal average at given height. The approach has its limitations, since dispersive terms can not be quantified.

The large number of successful runs (≈5000 h) allows performing the procedure for different stability classes. Stability was determined at tower top by z'/L, where z' is a scaling length (see 4.1) and L the Obukhov length.

Terms *Ps*, *Pb*, *Tt* and local rate of change have all been directly measured and aggregated by using the above averaging procedure for hourly blocks. Runs where all six instruments provide simultaneously error-free data are taken into statistics. All calculations have been simplified under the assumption of horizontal homogeneity in a larger scale (neighbourhood scale, 10^2 m). Vertical gradients have been approximated by the local derivative of a parametric cubic spline interpolation with the lower boundary set to zero at $z/h = 0$ and a relaxed upper boundary at $z/h = 2.17$. Local rate of change over the hourly blocks is typically on the order of 10^4 lower compared to the other terms and is neglected.

Dissipation rate of turbulent kinetic energy ε has been derived from the inertial subrange of longitudinal velocity spectra (see section 4.4). Spectra were calculated for 64 bands, using linearly detrended data over one hour blocks.

Tv is supposed to be negligible. Hence, a residual term incorporates mainly *Tp*, *Pd*, and *Td* and in the lower canyon additionally *Pt*. This residual term is further labeled *R*.

4 RESULTS

4.1 Scaling Length

In surface layer scaling, the dominant length scale is the distance above ground z (or z-z_d). This scaling fails in the canopy layer and in the lower parts of the roughness sublayer, because turbulence properties are dependent on characteristics of the roughness elements and not on height anymore. Table 2 illustrates that peak frequencies in TKE spectra T_{TKE} and Eulerian length scales Λ_{TKE} of turbulent fluctuations in the four lowest levels do not vary significantly with height. Therefore, in analogy to plant canopy studies, the preferred length scale is the mean building height h. This scaling is more appropriate in the canopy layer, however, the scales in the narrow street canyon are not well described by h and the h-scaling does not cope for the transition to the inertial sublayer above the roofs, where surface layer scaling applies. As an alternative, values can be scaled by z', where $z' = \max(z\text{-}z_d, y/2)$. In a deep street canyon, the largest eddy that fits into has a radius of $y/2$ where y is the canyon width.

Tab. 2: Characteristic peak frequency (T_{TKE}) and length scale (Λ_{TKE}) determined from individual TKE-spectra (n= 5474 h) for cases with a kinematic heat flux < 0.05, in comparison to the scaling lengths *h* and *z'*.

z/*h*	T_{TKE}	Λ_{TKE}	*h*	*z'*
2.17	25 sec	45 m	14.6 m	21.5 m
1.53	19 sec	27 m	14.6 m	12.1 m
1.23	20 sec	21 m	14.6 m	7.7 m
1.01	22 sec	18 m	14.6 m	5.5 m
0.77	31 sec	23 m	14.6 m	5.5 m
0.25	20 sec	16 m	14.6 m	5.5 m

4.2 Shear production of TKE

The vertical profile of mean horizontal wind throughout the urban roughness sublayer is shown in Fig 2a. Well above the roofs, the wind profile follows the logarithmic law. In the region around the mean building height, an elevated shear layer forms, characterized by an inflection point at ~1.1*h*. The inflected velocity profile produces an instability, which is associated with high vorticity, high drag and high turbulent kinetic energy in the region just around roof top.

It is no surprise, that in the layer just around the roofs, gradients are significantly stronger for flow situations with an overall wind direction perpendicular to the street canyon, compared to situations with wind along to the canyon axis (Fig 2a). In flow situations perpendicular to the canyon axis, a second wind speed maximum is observed at canyon floor. This wind speed maximum is a consequence of a simple vortex, which is observed in average in the street canyon (height to width ratio of 1). The vortex results in a dominating vertical mean wind in the middle part of the canyon and mainly horizontal winds at canyon floor. Vertical mean wind in the canyon is less important in along-canyon flow situations.

For most flow situations, local Reynolds stress shows its maximum well above the mean building height at 1.55*h*, and is again the slightly decreasing above (Fig 2b). This is in agreement with other field experiments (Rotach, 1993; Feigenwinter et al. 1999). Flow situations that are inclined to the canyon's axis are additionally characterized by a rotation of the mean wind direction with height and a channeling into the canyon. This results in further lateral contributions to the momentum flux, especially around roof-top. Therefore, the calculation of *Ps* was done taking lateral contributions into account.

Shear production of TKE (*Ps*) is shown in Fig 2d. Its magnitude is highest at 1.25*h* (Fig. 2d) and does not depend strongly on wind direction of the approaching flow**.** Above roof-level, shear production is by far the most important source for TKE (Fig. 3). It decreases rapidly inside the street canyon, both in absolute and relative numbers. At the zeroplane displacement height (0.7h) it becomes nearly zero. Higher wind speeds in the canyon under along canyon flow result in a small second maximum at canyon floor (Fig. 2d).

Recently, LES simulations demonstrated that the dispersive effects, which can not be directly measured with the current setup, may be relevant in the upper part of the urban canopy layer (Kanda *et al.*, 2004).

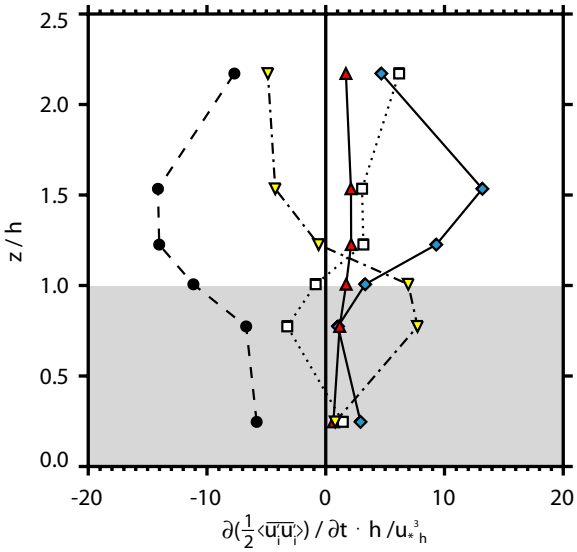

Fig. 3: Profiles of measured TKE budget terms. Shown are mean values of all stabilities using the averaging procedure described in section 3. All terms have been normalized by global h / u_{*h}^3 to be comparable to previous studies (n = 3317 h)

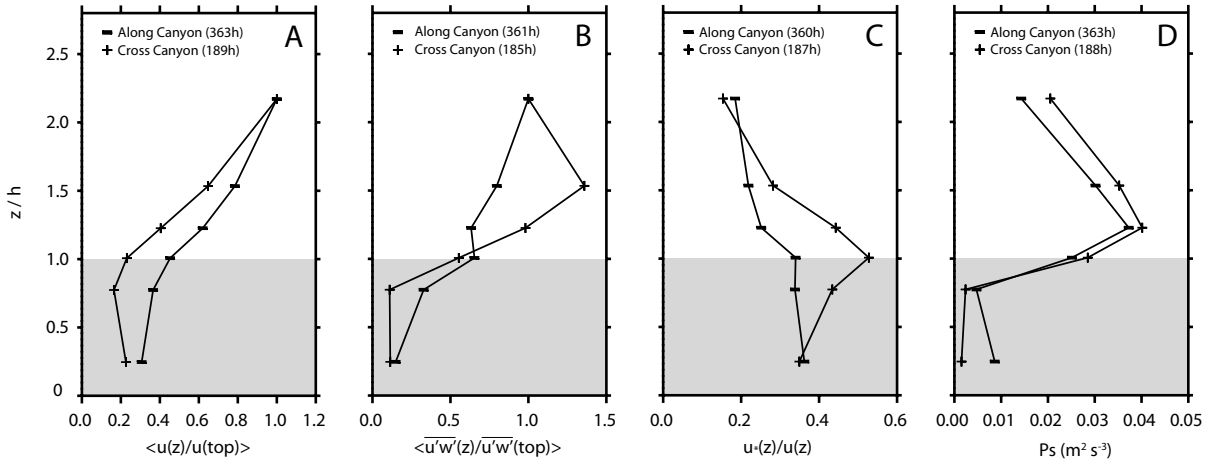

Fig. 2: Difference between flow directions along and perpendicular to the canyon's axis for the vertical profile of mean wind (A), local Reynolds stress (B), the square of the local drag coefficient (C), and average shear production of TKE in $m^2 s^{-3}$ (D). Shown are median values of all neutral runs.

Tab. 3: Characteristics of the buoyant production term for all stabilities and flow situations (n ≈ 3709h)

z/*h*	*Median* |*Pb*/*Ps*|	Cases with |*Pb*| > |*Ps*|	Cases with *Pb* < 0
2.17	0.28	26.9 %	9.8 %
1.53	0.13	16.8 %	6.4 %
1.23	0.12	8.8 %	6.6 %
1.01	0.27	25.3 %	6.7 %
0.77	0.71	41.5 %	9.2 %
0.25	0.30	22.2 %	14.6 %

4.3 Buoyancy production / destruction of TKE

Over a compact and densely built-up urban surface, mainly roof areas contribute to buoyant production. In absolute values, buoyant production of TKE is negligible within the canyon. Above the roofs, buoyancy production is typically five to ten times less important than shear production. The lower importance of the buoyant production term results in a dominating neutral and slightly unstable stratification in the urban roughness sublayer.

Highest absolute buoyant production rates are found during summer days, when heat fluxes are large and typically in the order of 300-400 Wm^{-2}. Figure 6 illustrates, that for unstable cases at tower top (z'/L < -1), buoyant production is typically half the magnitude of shear production above the roofs, but less relevant close to the roofs.

Situations when the buoyant term is a sink are rarely observed (Tab. 3). In the majority of all nights, the turbulent flux of sensible heat transports small amounts of energy away from the surface (5-10 W m^{-2}), a consequence of a strong release of heat stored in building materials (Christen and Vogt, 2004).

4.4 Dissipation rate of TKE

Dissipation was deduced from the inertial subrange (IS) of longitudinal velocity spectra using Kolmogorov's similarity approach and Taylor's hypothesis (Panofsky and Dutton, 1984):

$$\epsilon = \frac{2\pi n}{\overline{u}} \left(\frac{n S_u(n)}{\alpha_u} \right)^{3/2} \quad (2)$$

α_u is the Kolmogorov constant for u, n the frequency in s^{-1}, and S_u the spectral energy of the longitudinal velocity spectra. Calculations were done in bands between 0.1 and 1 s^{-1}, which were identified most appropriate, since higher frequencies are contaminated by back-folding and limited by instrument path length.

A correct estimation of ε is only achieved if (i) an undisturbed IS with local isotropy exists and (ii) the Taylor hypothesis is applicable. From studies in plant canopies it is known that effects like 'spectral shortcut' - a direct bypass of large scale turbulent kinetic energy to small scales by small canopy elements - may significantly alter spectra in high frequency bands. In a non-vegetated urban canopy such effects are supposed to be less relevant, since the highest spectral densities in size of roughness elements (10^{-1} to 10^{-2} m^{-1}) are larger than the corresponding wavenumbers in the IS (10^{-1} to 10^{0} m^{-1}). However we can not exclude the possibility of an overlapping of these two scales, and the range where ε is determined would then be slightly contaminated by kinetic energy directly produced in this small scale overlap region.

Critical for the dissipation calculation in the urban canopy layer may be the applicability of the Taylor hypothesis. If temporal variations in a moving frame of

Tab. 4: Average properties relevant for the calculation of ε for all stabilities and situations (n ≈ 5000 h). IS refers to the theoretical inertial subrange values.

z/*h*	Turbul. Intensity σ_u / u	IS Slope $\frac{\partial(\ln(S(k_1)))}{\partial(\ln(\kappa))}$	Ratio S_w / S_u	normal. Error $\frac{\frac{1}{N}\sum_{i=0}^{N}(\varepsilon_i - \varepsilon)^2}{\varepsilon}$
2.17	0.45	-1.63	1.14	12.8 %
1.53	0.52	-1.64	1.07	13.6 %
1.23	0.51	-1.62	1.03	14.0 %
1.01	0.48	-1.60	1.15	15.2 %
0.77	0.40	-1.59	1.05	15.3 %
0.25	0.40	-1.52	1.05	19.5 %
IS		-5/3	4/3	0%

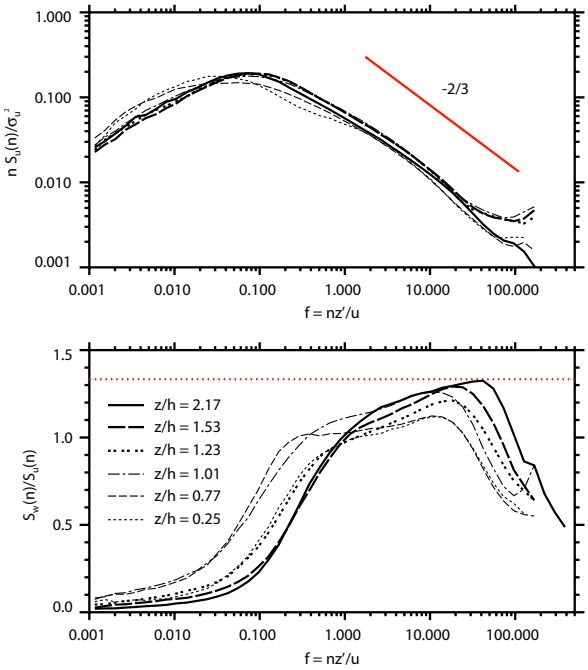

Fig. 4: Longitudinal velocity spectra with the inertial subrange slope indicated (top) and ratio S_w/S_u (bottom) for all runs with neutral stability.

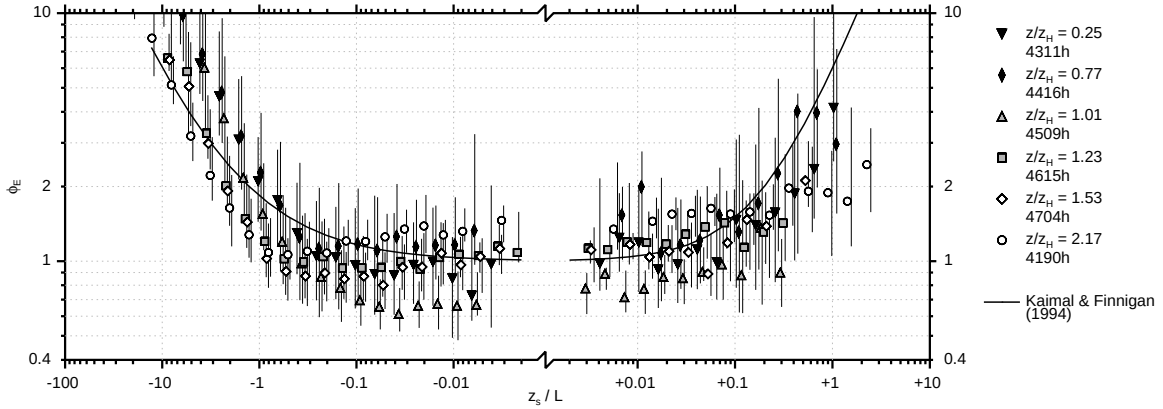

Fig. 5: Local scaled ϕ_ε in dependence of local stability determined by z'/L. Error bars indicate the range from the 25% quartile to the 75% quartile.

reference are strong and different wavenumbers are transported in different velocities, the Taylor hypothesis fails (Wyngaard and Clifford, 1977). This is not unlikely, because the strong wind shear creates turbulence intensities that are typically around 0.5 (Tab. 4), a value usually given as the threshold, above which Taylor's hypothesis becomes inapplicable (Willis and Deardorff, 1976). And, a strong pressure transport term could result in different propagation velocities for different wavenumbers.

The IS Slope was calculated as the average slope of the longitudinal spectra converted to wavenumbers in the IS (Tab. 4). At all measurement levels, the slope is slightly lower than the theoretical value of -5/3, which is interpreted as an indicator that small production rates still exist in this range. Moreover, the ratio S_w/S_u is below the theoretical value for local isotropy (4/3) (Fig. 4). Both values suggest an increase of IS-contamination with decreasing height. However, the values show that the contamination levels are still small compared to the energy passed down in the cascade, and therefore dissipation is affected by small errors, but a calculation is not impossible per se. The normalized error in Tab. 4 can be interpreted as the quality of estimating the -5/3 slope fit. It is calculated as the RMS deviation of a band individual ε_i relative to the average ε of all bands (N=13). Dissipation rates have only been calculated for runs with an IS-slope between -1.4 and -1.8.

The resulting dissipation rates are highest at roof top and decrease in both directions. Figure 5 illustrates the locally scaled $\phi_\varepsilon = kz'\varepsilon/u_*^3(z)$. Local scaling explains dissipation as a function of only z', (local) u_*, and (local) kinematic heat flux. Any transport terms are neglected. Transport terms are supposed to be small or to counterbalance each other as observed in the surface layer (McBean and Elliott, 1975). As a consequence, local dissipation is believed to only depend on production by shear and buoyancy.

In levels well above roof top, this local scaling results in acceptable estimations. This is mainly because transport terms *Tt* and *Pt* are of opposite sign. Close to roof top (grey triangles) ϕ_ε is systematically underestimated by the local scaling approach, because large amounts of TKE are exported by *Tt* and *Tp* from this region and are not anymore available for dissipation (see Section 4.5). On the other hand, in the upper canyon, dissipation is underestimated because of the import of TKE, mainly by *Tt*. In order to accurately predict ε in the urban roughness sublayer,

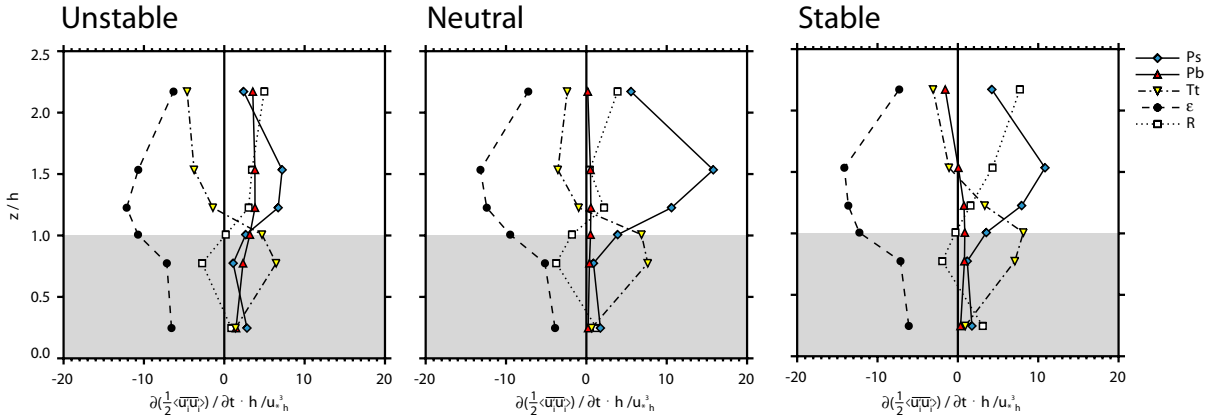

Fig. 6: Normalized and averaged TKE-Budget for different stabilities. Stability was determined at tower top with the following ranges: Unstable: -10 < z'/L < -1 (854 h), Neutral: -0.1 < z'/L < +0.1 (971 h), Stable: +0.1 < z'/L < 10 (82 h).

transport terms have to be included.

4.5 Turbulent Transport of TKE

Over the whole vertical profile the TKE budget is not in local equilibrium, thus the locally produced turbulent kinetic energy does not equal local dissipation. As a consequence, TKE has to be vertically relocated by transport processes, mainly *Tt*, and *Tp*, and possibly *Td*.

The only transport term that can be measured directly is the turbulent transport of TKE (*Tt*). The results show, that excess TKE from the region above rooftop ($z/h > 1.2$) is transported down into the upper part of the street canyon (Fig. 3 and 6). In the upper canopy part, *Tt* is the most important source of TKE and 10 times more important than local shear and buoyant production together. Its magnitude is less relevant in the canyon floor. This pattern is similarly reported form observations in forests (Leclerc *et al.*, 1990; Meyers and Baldocchi, 1991)

Roth and Oke (1993) suggested in their analysis of a suburban dataset, that large organized structures are involved in the relocation and transfer of turbulent kinetic energy. The importance of these structures in the roughness sublayer has been further underlined by Oikawa and Meng (1995) and Feigenwinter and Vogt (2004).

Quadrant analysis of the present dataset indicates a highly asymmetric turbulent exchange for *u'w'* at roof top and in the upper canyon region, with mainly sweeps, i.e. stress fractions in the 4^{th} quadrant dominate over stress fractions in the 2^{nd} quadrant. At the topmost measurement level ($z/h > 2$), the pattern changes and ejections dominate over sweeps. These sweeps become even more important above, as measurements at a 75m tower 200 m to the South-East of the present site suggest (Feigenwinter *et al.*, 1999).

4.6 Residual Term

Pressure transport is likely the most important non-measured term. Therefore the residual term is mainly interpreted as pressure transport. The results have to be treated carefully, since a residual term includes all errors of the measurements and all simplifications.

Pressure disturbances are primarily created in the region around roof top. They relocate TKE from this region and put it into higher layers of the roughness sublayer and also down into the very bottom of the street canyon (Fig. 3 and 6). This pattern is in qualitative agreement with the few measurements in plant canopies (Maitani and Seo, 1985; Shaw *et al.*, 1990) and also with LES studies of model canopies (Dwyer *et al.*, 1997). The results from the LES study suggest that thermal stability affects *Tp* by increasing it substantially under unstable stratifications. Such indications are not found in the present data, where all stabilities result in a similar pattern and magnitude of the transport terms (Fig. 6).

In the upper part of the profile, the pressure transport and turbulent transport are of opposite sign, which corresponds to the observations in the surface layer.

In the bottom of the street canyon, the traffic produced turbulent kinetic energy *Pt* is part of the residual term. However, no correlation is found between the magnitude of the residual term and the traffic load in the street canyon. Traffic load was counted over 4 weeks during the measurement campaign. The moderate traffic load (2000 vehicles per day) and the low speed limit (30 km/h) likely do not strongly influence canyon turbulence.

ACKNOWLEDGEMENTS

The Swiss Federal Office for Education and Science provides funding of this study (C00.0068). Many thanks go to the students and staff at University of Basel and ETH Zürich who helped setting up and maintaining the tower.

REFERENCES

BUBBLE website: http://www.unibas.ch/geo/mcr/Projects/BUBBLE/

Christen A, Vogt R (2004): Energy and radiation balance of a central European city. Accepted by: *Int. J. Climatol.* May 2004.

Di Sabatino S, Kastner-Klein P, Berkowicz R, Britter RE, Fedorovich E (2003): The modelling of turbulence from traffic in urban dispersion models - Part I: Theoretical considerations. *Env. Fluid. Mech.* 3 (2): 129-143.

Dwyer MJ, Patton EG, Shaw RH (1997): Turbulent kinetic energy budgets from a large-eddy simulation of airflow above and within a forest canopy. *Bound.-Layer Meteorol.* 84: 23-43.

Feigenwinter C., Vogt R, Parlow E (1999): Vertical structure of selected turbulence characteristics above an urban canopy. *Theor. Appl. Climatol.* 61. 51-63.

Feigenwinter C, Vogt R (2004): Detection and analysis of coherent structures in urban turbulence. Submitted to: *Theor. Appl. Climatol.*

Finnigan JJ (2000): Turbulence in Plant Canopies. *Annu. Rev. Fluid Mech.,* 22: 519-571.

Leclerc MY, Beissner KC, Shaw RH, den Hartog G and Neumann HH (1990): The influence of atmospheric stability on the budgets of the Reynolds stress and turbulent kinetic energy within and above a deciduous forest. *J. Appl. Climatol.* 29. 916-933.

Kanda M, Moriwaki R, Kasamatsu F (2004): Large-eddy simulation of turbulent organized structures within and above explicitly resolved cube arrays. *Bound.-Layer Meteorol.* 112(2): 343-368.

Maitani T, Seo T (1985): Estimates of velocity-pressure and velocity pressure gradient interactions in the surface layer above plant canopies. Bound.-Layer Meteorol. 33. 51-60.

McBean GA, Elliott JA (1975): Vertical transports of kinetic-energy by turbulence and pressure in boundary-layer *J. Atmos. Sci.* 32 (4): 753-766.

Meyers TP, Baldocchi DD (1991): The budgets of turbulent kinetic energy and Reynolds stress within and above a deciduous forest. *Agric. Forest Meteorol.* 53. 207-222.

Oikawa S, Meng Y (1995): Turbulence characteristics and organized motion in a suburban roughness sublayer. *Bound.-Layer Meteorol.* 74: 289-312.

Panofsky HA, Dutton JA (1984): Atmospheric turbulence. John Wiley & Sons, New York, pp. 397

Raupach MR, Shaw RH (1982): Averaging procedures for flow within vegetation canopies. *Bound.-Layer Meteorol.*, 22: 79–90, 1982.

Rotach MW (1993): Turbulence close to a rough urban surface. Part I: Reynolds stress. *Bound.-Layer Meteorol.* 66: 75-92.

Rotach MW (1999): On the influence of the urban roughness sublayer on turbulence and dispersion *Atmos. Environ.* 33 (24-25): 4001-4008.

Rotach MW, Vogt R, Bernhofer C, Batchvarova E, Christen A, Clappier A, Feddersen B, Gryning S-E, Martucci G, Mayer H, Mitev V, Oke TR, Parlow E, Richner H, Roth M, Roulet YA, Ruffieux D, Salmond J, Schatzmann M, Voogt J (2004): BUBBLE – a Major Effort in Urban Boundary Layer Meteorology. Submitted to: *Theor. Appl. Climatol.*

Roth M, Oke TR (1993): Turbulent transfer relationships over an urban surface .1. Spectral characteristics. *Quart. J. Roy. Meteor. Soc.* 119: 1071-1104.

Shaw RH, Paw U KT, Zhang XJ, Gao W den Hartog G, Neumann HH (1990) Retrieval of turbulent pressure fluctuations at the ground surface beneath a forest. Bound.-Layer Meteorol. 50. 319-338.

Vogt R, Feigenwinter C (2004): Sonic anemometers tested in a wind tunnel. *26th AMS Conference on Agricultural and Forest Meteorology.* 23—27 August Vancouver BC, Canada.

Willis GE, Deardorff JW (1976): On the use of Taylor's hypothesis for diffusion in the mixed layer. *Quart. J. Roy. Meteor. Soc.* 102. 817-822.

Wyngaard JC, Clifford SF (1977): Taylor's hypothesis and high frequency turbulence spectra. *J. Atmos. Sci.* 34. 922-929.